NORGES TEKNISK-NATURVITENSKAPELIGE
UNIVERSITET

Evaluation of flux integral outputs for the reduced basis method

by

Jens L. Eftang and Einar M. Rønquist

PREPRINT
NUMERICS NO. 11/2008

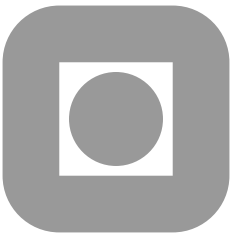

NORWEGIAN UNIVERSITY OF
SCIENCE AND TECHNOLOGY
TRONDHEIM, NORWAY

This report has URL
http://www.math.ntnu.no/preprint/numerics/2008/N11-2008.pdf
Address: Department of Mathematical Sciences, Norwegian University of Science and Technology, N-7491 Trondheim, Norway.

Evaluation of flux integral outputs for the reduced basis method

Jens L. Eftang and Einar M. Rønquist

1st December 2008

Abstract

In this paper, we consider the evaluation of flux integral outputs from reduced basis solutions to second-order PDE's. In order to evaluate such outputs, a lifting function $v^\star$ must be chosen. In the standard finite element context, this choice is not relevant, whereas in the reduced basis context, as we show, it greatly affects the output error. We propose two "good" choices for $v^\star$, and illustrate their effect on the output error by examining a numerical example. We also make clear the role of $v^\star$ in a more general primal-dual reduced basis approximation framework.

1 Introduction

For many practical applications, one is interested in certain physical averages, or *outputs of interest*, which can be defined as functionals of the solution to a partial differential equation (PDE) that describes an underlying physical problem. For example, the output of interest may be the average heat flux through (or average temperature on) a surface, or the average force acting on a wall due to fluid flow. In this paper, we are concerned with outputs of *flux integral type*, i.e., outputs that can be written as surface integrals of the normal derivative of the solution to the underlying PDE. We consider second-order equations, for which it is possible to evaluate flux integral outputs directly via the weak problem formulation, and in particular without the need for any numerical differentiation.

Mathematically, we consider a weakly written problem defined on a domain Ω: Find $u \in X(\Omega)$ such that

$$a(u, v) = f(v), \quad \forall v \in X(\Omega), \tag{1}$$

where a is a coercive, continuous and for simplicity also symmetric bilinear form derived from some second-order differential operator, f is a linear and bounded functional, $X(\Omega) = \{v \in H^1(\Omega) : v|_{\Gamma_\mathrm{D}} = 0\}$ is our exact space, and $\Gamma_\mathrm{D} \subset \partial\Omega$ denotes the parts of the boundary of Ω on which we impose (for

simplicity homogeneous) Dirichlet boundary conditions. As usual, $H^1(\Omega)$ denotes the Sobolev space of functions with square integrable first order derivatives. Henceforth, the Ω-dependence of our spaces is understood when no ambiguity may arise.

Our output of interest shall be the integral of the flux through $\Gamma_{\mathrm{D}}^0 \subseteq \Gamma_{\mathrm{D}}$. We thus define the output functional

$$\tilde{l}^{\mathrm{out}}(w) \equiv \int_{\Gamma_{\mathrm{D}}^0} \frac{\partial w}{\partial n} \, \mathrm{d}s, \tag{2}$$

where $\partial/\partial n$ denotes the outward normal derivative and s is the surface measure on Γ_{D}. When solving e.g. Poisson or Helmholtz problems with the finite element (FE) method, it is preferable [1, 2, 5, 9] to evaluate flux integral outputs through the functional

$$l^{\mathrm{out}}(w) \equiv a(w, v^\star) - f(v^\star), \tag{3}$$

where $v^\star \in H^1$ is any function that is equal to unity on Γ_{D}^0 and equal to zero on $\Gamma_{\mathrm{D}} \setminus \Gamma_{\mathrm{D}}^0$. Of course, even though (2) and (3) make sense for any $w \in X$, they are only of interest for $w \approx u$, where u is the solution of (1). One way to derive (3), is to recast the original problem (1) as a "Neumann problem" for which there are no restrictions on the test functions on Γ_{D}^0. Thus, if we suppose (1) is a Poisson or Helmholtz problem, this modified problem reads: Find $u \in \tilde{X}$ such that

$$a(u, v) = f(v) + \int_{\Gamma_{\mathrm{D}}^0} \frac{\partial u}{\partial n} v \, \mathrm{d}s, \quad \forall v \in \tilde{X}, \tag{4}$$

where $\tilde{X} = \{v \in H^1 : v|_{\Gamma_{\mathrm{D}} \setminus \Gamma_{\mathrm{D}}^0 = 0}\} \supset X$. Moving $f(v)$ to the left hand side and choosing $v = v^\star \in \tilde{X}$, we see that $\tilde{l}^{\mathrm{out}}(u) = l^{\mathrm{out}}(u)$.

Suppose we solve (1) numerically to obtain a FE approximation to u, $u^{\mathcal{N}} \in X^{\mathcal{N}}$, satisfying

$$a(u^{\mathcal{N}}, v) = f(v), \quad \forall v \in X^{\mathcal{N}}. \tag{5}$$

Here, $X^{\mathcal{N}} \subset X$ is our discrete FE space with $\mathcal{N}$ degrees of freedom. Our output of interest can now be evaluated in two ways, either as $\tilde{l}^{\mathrm{out}}(u^{\mathcal{N}})$ or as $l^{\mathrm{out}}(u^{\mathcal{N}})$. In the latter case, we assume $u^{\mathcal{N}}$ is a good approximation to u, and we thus substitute $u^{\mathcal{N}}$ for u and $\approx$ for $=$ in (4). With $v = v^\star$, we get $l^{\mathrm{out}}(u^{\mathcal{N}}) \approx \int_{\Gamma_{\mathrm{D}}^0} \frac{\partial u^{\mathcal{N}}}{\partial n} \, \mathrm{d}s$. Hence, in general, $l^{\mathrm{out}}(u^{\mathcal{N}}) \neq \tilde{l}^{\mathrm{out}}(u^{\mathcal{N}})$.

We shall refer to $v^\star$ as a *flux lifting function*, and we shall denote the set of possible such functions as $V^\star$, i.e.,

$$V^\star \equiv \{v \in H^1 : v|_{\Gamma_{\mathrm{D}} \setminus \Gamma_{\mathrm{D}}^0} = 0, v|_{\Gamma_{\mathrm{D}}^0} = 1\}. \tag{6}$$

In [1, 2], $v^\star$ is called an *extraction function*, and the method described above for flux integral output evaluation is an example of an *extraction method*, as

similar techniques may be used for other types of output. In [9], the method – although with emphasis on pointwise quantities, rather than on surface integrals – is called *the consistent Galerkin FEM*. In any event, $l^{\text{out}}(u^{\mathcal{N}})$ typically converges to $l^{\text{out}}(u)$ quadratically with the energy-norm error of the field variable, $\|u - u^{\mathcal{N}}\|$, in contrast to $\tilde{l}^{\text{out}}(u^{\mathcal{N}})$, which exhibits only linear convergence [2, 5]. Another advantage of l^{out} over $\tilde{l}^{\text{out}}$ is that the former requires no calculation of normal derivatives, which is particularly convenient in higher dimensions and for problems on domains with curved boundaries.

Aside from the essential boundary condition in (6), we have not made any particular choice for $v^\star \in H^1$. In fact, within a standard finite element framework, this choice is not a big issue due to the richness of the approximation spaces used [2, 5]. (It is, however, important that $v^\star$ be a smooth function on each element [1].) In contrast, as we will show numerically and theoretically, one should take a little more care when evaluating flux integral outputs by way of the method described above within the *reduced basis* (RB) framework. Confer e.g. [14] for a thourough introduction to RB methods.

In the next section, we shall consider a very simple numerical example that illustrates how l^{out} may be superior to $\tilde{l}^{\text{out}}$ in terms of numerical accuracy within the FE framework. In Section 3, we first briefly review the RB method and then elaborate on the discrepancy between the FE and RB methods with respect to the choice of $v^\star$. We then propose two "good" choices for $v^\star$ to use in the RB context. We also make clear the role of $v^\star$ in the more general primal-dual RB approximation procedure that is used to speed up the convergence of non-compliant problems [12, 14]. In Section 4, we remain in the RB context and illustrate the effect of different $v^\star$'s by examining yet another numerical example, and in Section 5 we end our discussion with some concluding remarks.

2 Flux Output Evaluation: a 1D Example

We consider a one-dimensional Helmholtz problem on $\Omega = (0, 2)$ with homogeneous Dirichlet boundary conditions. The weak formulation of the problem reads: Find $u \in H^1_0$ such that

$$\underbrace{\int_0^2 \left(\frac{\partial u}{\partial x}\frac{\partial v}{\partial x} + uv \right) \mathrm{d}x}_{=a(u,v)} = \underbrace{\int_0^2 qv \, \mathrm{d}x}_{=f(v)}, \quad \forall v \in H^1_0, \tag{7}$$

where we choose the source term $q(x) = x^{2/3}$ to make u weakly singular. Our output of interest is the derivative of u at $x = \Gamma^0_{\text{D}} = \{2\}$, and our two

output functionals now reduce to

$$\tilde{l}^{\text{out}}(w) = \left.\frac{\partial w}{\partial x}\right|_{x=2} \tag{8}$$

and

$$l^{\text{out}}(w) = a(w, v^\star) - f(v^\star), \tag{9}$$

where $v^\star \in V^\star$.

With a spectral (high order polynomial) method, we discretise (7) and find $u^{\mathcal{N}} \in X^{\mathcal{N}}$ such that

$$a(u^{\mathcal{N}}, v) = f(v), \quad \forall v \in X^{\mathcal{N}}, \tag{10}$$

where

$$X^{\mathcal{N}} = \{v \in \mathbb{P}^{\mathcal{N}+1} : v_{\Gamma_{\text{D}}} = 0\} \tag{11}$$

is our discrete space. Here, $\Gamma_{\text{D}} = \{0, 2\}$ and $\mathbb{P}^{\mathcal{N}+1}$ denotes the space of polynomials of degree $\mathcal{N}+1$ (note that $\dim(X^{\mathcal{N}}) = \mathcal{N}$ due to the Dirichlet boundary conditions).

We shall also consider the dual problem: Find $\psi \in H_0^1$ such that

$$a(v, \psi) = -a(v, v^\star), \quad \forall v \in H_0^1. \tag{12}$$

The spectral discretisation of (12) reads: Find $\psi^{\mathcal{N}} \in X^{\mathcal{N}}$ such that

$$a(v, \psi^{\mathcal{N}}) = -a(v, v^\star), \quad \forall v \in X^{\mathcal{N}}. \tag{13}$$

Note that the linear functional part of l^{out}, which is bounded, enters on the right hand side in the dual problem (with a minus sign). Thus, $v^\star$ also plays the role of a Dirichlet lifting function for the dual problem, with Dirichlet data equal to unity on Γ_{D}^0 (i.e. at $x = 2$). Also note that the dual problem exhibits no (singular) source term. Provided $v^\star$ is smooth (deliberately choosing $v^\star$ singular seems somewhat peculiar), we expect ψ to be a smooth function and thus the convergence of $\psi^{\mathcal{N}}$ to ψ to be of infinite order.

We are interested in the errors in the output of interest, which we define for each of our two output functionals as

$$\tilde{e}^{\mathcal{N},\text{out}} \equiv \left| \frac{\partial u}{\partial x}\Big|_{x=2} - \tilde{l}^{\text{out}}(u^{\mathcal{N}}) \right|, \tag{14}$$

and

$$e^{\mathcal{N},\text{out}} \equiv \left| \frac{\partial u}{\partial x}\Big|_{x=2} - l^{\text{out}}(u^{\mathcal{N}}) \right| = \left| l^{\text{out}}(u) - l^{\text{out}}(u^{\mathcal{N}}) \right|, \tag{15}$$

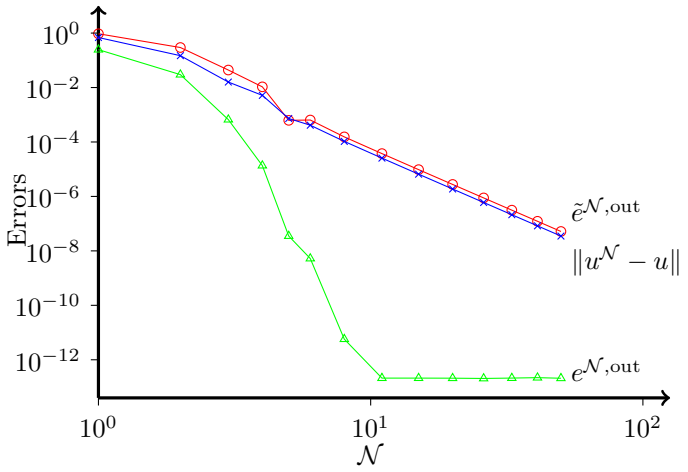

Figure 1: Energy error ($\times$) and output errors $e^{\mathcal{N},\text{out}}$ ($\triangle$) and $\tilde{e}^{\mathcal{N},\text{out}}$ ($\circ$) for increasing polynomial degree, $\mathcal{N}$, of the underlying numerical solution.

respectively. For $e^{\mathcal{N},\text{out}}$, we deduce that

$$\begin{aligned} e^{\mathcal{N},\text{out}} &= |a(u - u^{\mathcal{N}}, v^\star)| \\ &= |a(u - u^{\mathcal{N}}, \psi)| \\ &= |a(u - u^{\mathcal{N}}, \psi - \psi^{\mathcal{N}})| \\ &\leq \|u - u^{\mathcal{N}}\| \|\psi - \psi^{\mathcal{N}}\|, \end{aligned} \tag{16}$$

by using the definition of $e^{\mathcal{N},\text{out}}$, the fact that $u^{\mathcal{N}} - u \in H_0^1$ and the definition of the dual problem (12), Galerkin orthogonality of $u - u^{\mathcal{N}}$ and the Cauchy-Schwarz inequality, respectively. Here, $\|\cdot\| = \sqrt{a(\cdot,\cdot)}$ denotes the energy norm. A consequence of this estimate is that if ψ happens to be a smooth function, $e^{\mathcal{N},\text{out}}$ will decay exponentially with $\mathcal{N}$, even if u is singular. Note that in practice, we never actually compute the discrete solution $\psi^{\mathcal{N}}$ to the dual problem.

In Figure 1, we plot the energy norm error $\|u - u^{\mathcal{N}}\|$ and the output errors $\tilde{e}^{\mathcal{N},\text{out}}$ and $e^{\mathcal{N},\text{out}}$ for $1 \leq \mathcal{N} \leq 50$. As our flux lifting function, we have made the choice $v^\star = x/2$. As expected, the error $\|u - u^{\mathcal{N}}\|$ decays algebraically, while $e^{\mathcal{N},\text{out}}$ decays at an infinite rate due to the smoothness of ψ. We note that for our simple one-dimensional problem, $\tilde{e}^{\mathcal{N},\text{out}}$ decays as fast as the error $\|u - u^{\mathcal{N}}\|$.

Let us make a few remarks concerning the above results. Firstly, since $q(x) = x^{2/3}$ is not a smooth function over Ω, the integrand on the right hand side of the primal problem is singular. As a result, we must make sure that we compute the integral $f(v)$ with sufficient accuracy in order to maintain the exponential convergence of the output. Otherwise, $u^{\mathcal{N}}$ would carry an additional numerical integration error compromising Galerkin orthogonality,

which we exploited in the error bound (16). In our numerical experiment, we have computed the integral $f(v)$ using Gauss-Lobatto-Legendre (GLL) quadrature [4] over $n_q \gg \mathcal{N}+1$ quadrature points.

Secondly, we would expect similar results were we to use a linear finite element method. In fact, if u_h denotes a linear FE approximation to u on a mesh with elements of size h, we would from standard error estimates [13] expect convergence of order $\mathcal{O}(h^2)$ for the output $l^{\text{out}}(u_h)$, and of order $\mathcal{O}(h)$ for the energy norm $\|u-u_h\|$ (note that for our particular problem, the singularity in u is weak enough that full linear convergence is achieved). Based on the preceeding results, we would also expect convergence of order $\mathcal{O}(h)$ for the output $\tilde{l}^{\text{out}}(u_h)$. Indeed, such results are presented in [5] for a very similar example as the one discussed above.

Thirdly, as noted in [2], any two choices of $v^\star \in (V^\star \cap \tilde{X}^{\mathcal{N}})$ produce the same result for $l^{\text{out}}(u^{\mathcal{N}})$. To see this, let $v_1^\star, v_2^\star \in (V^\star \cap \tilde{X}^{\mathcal{N}})$. Then $w^\star = v_1^\star - v_2^\star \in X^{\mathcal{N}}$, and

$$\left[a(u^{\mathcal{N}}, v_1^\star) - l(v_1^\star)\right] - \left[a(u^{\mathcal{N}}, v_2^\star) - l(v_2^\star)\right] = a(u^{\mathcal{N}}, w^\star) - l(w^\star) = 0, \quad (17)$$

by (10). A convenient choice for $v^\star$, then, is the function that is equal to unity at the node at $x=2$ and equal to zero at every other node (or, in the low-order finite element case, the function that is equal to unity at $x=2$ with support only on the element adjacent to the boundary). For this reason, we do not specifically emphasise our choice for $v^\star$ when considering outputs from FE approximations.

In the next section, we turn our focus to flux integral outputs in the Reduced Basis context.

3 Flux Output Evaluation within the Reduced Basis Framework

3.1 Reduced basis formulation

Within the reduced basis (RB) framework, one is interested in the solution of *parameterised* PDE's, and the corresponding outputs of interest, in the "real time" or "many query" situation [14]. The underlying PDE is configured by one or more parameters, governing e.g. boundary conditions, material or geometrical properties, or loads. Given any parameter vector $\boldsymbol{\mu} \in \mathcal{D}$, where $\mathcal{D} \subset \mathbb{R}^P$ is some admissible parameter domain, we consider the parameterised problem on a domain Ω: Find $u(\boldsymbol{\mu}) \in X$ such that

$$a(u(\boldsymbol{\mu}), v; \boldsymbol{\mu}) = f(v; \boldsymbol{\mu}), \quad \forall v \in X, \quad (18)$$

where $a(\cdot,\cdot;\boldsymbol{\mu})$ is a $\boldsymbol{\mu}$-dependent affine, coercive and continuous bilinear form originating from a second-order differential operator, and $f(\cdot;\boldsymbol{\mu})$ is a $\boldsymbol{\mu}$-dependent affine, linear and bounded functional (in addition, we still assume

for simplicity that $a(\cdot,\cdot;\boldsymbol{\mu})$ is symmetric). By *affine*, we here understand that, for all $v, w \in X$, we may expand $a(v, w; \boldsymbol{\mu})$ and $f(v; \boldsymbol{\mu})$ as

$$a(v, w; \boldsymbol{\mu}) = \sum_{q=1}^{Q_a} a^q(v, w)\Theta_a^q(\boldsymbol{\mu}), \quad f(v; \boldsymbol{\mu}) = \sum_{q=1}^{Q_f} f^q(v)\Theta_f^q(\boldsymbol{\mu}), \tag{19}$$

for finite numbers Q_a and Q_f, where the a^q and f^q are parameter independent bilinear and linear forms, respectively, and the Θ_a^q and Θ_f^q are parameter dependent functions.

We still impose homogeneous Dirichlet boundary conditions on $\Gamma_{\rm D} \subset \partial\Omega$, and take as our exact output of interest the flux integral

$$\tilde{s}(\boldsymbol{\mu}) = \int_{\Gamma_{\rm D}^0} \frac{\partial u(\boldsymbol{\mu})}{\partial n}\, {\rm d}s, \tag{20}$$

where $\Gamma_{\rm D}^0 \subseteq \Gamma_{\rm D}$.

Next, we define a "truth" finite element discretisation of (18) as: For $\boldsymbol{\mu} \in \mathcal{D}$, find $u^{\mathcal{N}}(\boldsymbol{\mu}) \in X^{\mathcal{N}}$ such that

$$a(u^{\mathcal{N}}(\boldsymbol{\mu}), v; \boldsymbol{\mu}) = f(v; \boldsymbol{\mu}), \quad \forall v \in X^{\mathcal{N}}. \tag{21}$$

By the appellation "truth", we here understand that $\mathcal{N}$ is chosen large enough that we cannot practically distinguish between the finite element solution, $u^{\mathcal{N}}(\boldsymbol{\mu})$, and the exact solution, $u(\boldsymbol{\mu})$. Correspondingly, our "truth" output of interest is

$$s^{\mathcal{N}}(\boldsymbol{\mu}) \equiv l^{\rm out}(u^{\mathcal{N}}(\boldsymbol{\mu}); \boldsymbol{\mu}) \equiv a(u_N(\boldsymbol{\mu}), v^\star; \boldsymbol{\mu}) - f(v^\star; \boldsymbol{\mu}). \tag{22}$$

Given a set of N wisely selected [14] parameter vectors $\boldsymbol{\mu}_1, \boldsymbol{\mu}_2, \ldots, \boldsymbol{\mu}_N \in \mathcal{D}$, we define our RB approximation space as

$$X_N = {\rm span}\{u^{\mathcal{N}}(\boldsymbol{\mu}_1), \ldots, u^{\mathcal{N}}(\boldsymbol{\mu}_N)\}. \tag{23}$$

The reduced basis problem now becomes: Given $\boldsymbol{\mu} \in \mathcal{D}$, find $u_N(\boldsymbol{\mu}) \in X_N$ such that

$$a(u_N(\boldsymbol{\mu}), v; \boldsymbol{\mu}) = f(v; \boldsymbol{\mu}), \quad \forall v \in X_N, \tag{24}$$

and evaluate the RB flux integral output

$$s_N(\boldsymbol{\mu}) \equiv l^{\rm out}(u_N(\boldsymbol{\mu}); \boldsymbol{\mu}) = a(u_N(\boldsymbol{\mu}), v^\star; \boldsymbol{\mu}) - f(v^\star; \boldsymbol{\mu}). \tag{25}$$

Note that we have assumed evaluation of the "truth" and RB flux integral outputs in (22) and (25), respectively, by using a flux lifting function $v^\star \in V^\star$, although we have not yet made any particular choice for $v^\star$.

Of interest within the RB context is the concept of a *compliant* problem. A problem is said to be compliant if, for all $\boldsymbol{\mu} \in \mathcal{D}$, *i)* the output

functional $l^{\text{out}}(\cdot;\boldsymbol{\mu})$ (more generally, in the case of $l^{\text{out}}(\cdot;\boldsymbol{\mu})$ affine, the linear functional part of $l^{\text{out}}(\cdot;\boldsymbol{\mu})$) is equal to the right-hand-side $f(\cdot;\boldsymbol{\mu})$ of (18), and *ii)* $a(\cdot,\cdot;\boldsymbol{\mu})$ is symmetric. In the compliant case, the error in the RB output of interest is *equal* to the square of the energy-norm error of the primary field variable [14].

In our case, $l^{\text{out}}(\cdot;\boldsymbol{\mu})$ as defined above is a non-compliant output functional since its linear functional part $a(\cdot,v^\star;\boldsymbol{\mu})$ is, in general different from the right-hand-side $f(\cdot;\boldsymbol{\mu})$ of (18), and that it is, strictly speaking, not linear, but affine, due to the translation term $f(v^\star;\boldsymbol{\mu})$. We make a comment in Section 4 on a very particular case in which $l^{\text{out}}(\cdot;\boldsymbol{\mu})$ is, in fact, compliant.

Due to the assumptions (19) on affinity (in functions of $\boldsymbol{\mu}$), a desirable offline-online computational approach for u_N and s_N may straightforwardly be developed [14]. The offline stage, which is performed only once, is computationally very costly, whereas the online stage – in which, given any new $\boldsymbol{\mu}\in\mathcal{D}$, the RB solution $u_N(\boldsymbol{\mu})$ and RB output of interest $s_N(\boldsymbol{\mu})$ are computed – is very fast. In particular, the computational complexity of the online stage is independent of $\mathcal{N}$, the number of degrees of freedom associated with the "truth" approximations $u^{\mathcal{N}}(\boldsymbol{\mu}_n)$, $1\le n\le N$.

Finally, we also define the now parameter dependent "energy" norm

$$\|\cdot\|_{\boldsymbol{\mu}} \equiv \sqrt{a(\cdot,\cdot;\boldsymbol{\mu})}, \tag{26}$$

and the equivalent parameter-independent X-norm

$$\|\cdot\|_X \equiv \sqrt{a(\cdot,\cdot;\bar{\boldsymbol{\mu}})}, \tag{27}$$

where $\bar{\boldsymbol{\mu}}\in\mathcal{D}$ is some fixed, preselected reference parameter.

3.2 Relevance of the flux lifting function

In Section 2, we saw that any two choices for $v^\star$ belonging to $(V^\star\cap\tilde{X}^{\mathcal{N}})$ produced the same output $l^{\text{out}}(u^{\mathcal{N}})$ within a standard FE framework. This is of course a consequence of the richness and generality of the FE space, $X^{\mathcal{N}}$. Within the RB framework however, the choice of flux lifting function does affect the numerical value of the output. To see this, let $v_1^\star, v_2^\star\in(V^\star\cap\tilde{X}^{\mathcal{N}})$, and define $w^\star\equiv v_1^\star - v_2^\star$. To emphasise a particular choice for $v^\star$, we write

$$s_N(\boldsymbol{\mu};v^\star) \equiv a(u_N(\boldsymbol{\mu}),v^\star;\boldsymbol{\mu}) - f(v^\star;\boldsymbol{\mu}). \tag{28}$$

Hence, the outputs corresponding to $v_1^\star$ and $v_2^\star$ are given by

$$s_N(\boldsymbol{\mu};v_1^\star) = a(u_N(\boldsymbol{\mu}),v_1^\star;\boldsymbol{\mu}) - f(v_1^\star;\boldsymbol{\mu}), \tag{29}$$

$$s_N(\boldsymbol{\mu};v_2^\star) = a(u_N(\boldsymbol{\mu}),v_2^\star;\boldsymbol{\mu}) - f(v_2^\star;\boldsymbol{\mu}), \tag{30}$$

respectively. But then,

$$\begin{aligned} s_N(\boldsymbol{\mu}; v_1^\star) - s_N(\boldsymbol{\mu}; v_2^\star) &= a(u_N(\boldsymbol{\mu}), v_1^\star; \boldsymbol{\mu}) - f(v_1^\star; \boldsymbol{\mu}) \\ &\quad - \big(a(u_N(\boldsymbol{\mu}), v_2^\star; \boldsymbol{\mu}) - f(v_2^\star; \boldsymbol{\mu})\big) \\ &= a(u_N(\boldsymbol{\mu}), w^\star; \boldsymbol{\mu}) - f(w^\star; \boldsymbol{\mu}), \end{aligned} \tag{31}$$

which by (24) is equal to zero for all $w^\star \in X_N$. However, for an arbitrary $w^\star \in X^{\mathcal{N}}$, $a(u_N(\boldsymbol{\mu}), w^\star; \boldsymbol{\mu}) - f(w^\star; \boldsymbol{\mu})$ is *nonzero*. Otherwise, $u_N(\boldsymbol{\mu})$ would have been identical to $u^{\mathcal{N}}(\boldsymbol{\mu})$, which is provably not the case for a general $\boldsymbol{\mu} \in \mathcal{D}$. In conclusion, the two evaluations $s_N(\boldsymbol{\mu}, v_1^\star)$ and $s_N(\boldsymbol{\mu}, v_2^\star)$ are not in general equivalent (unless $v_1^\star - v_2^\star$ happens to belong to X_N). Naturally, this raises the question of which $v^\star$ we should choose within the RB framework.

3.3 *A posteriori* error estimation

Before we proceed to our actual choices for "good" RB flux lifting functions, we shall consider the *a posteriori* error upper bound associated with the output $s_N(\boldsymbol{\mu})$. To arrive at such a bound, we first require a bound for the error in the field variable. We assume that we have available a lower bound $\alpha_{\mathrm{LB}}(\boldsymbol{\mu}) > 0$ for the coercivity constant of $a(\cdot, \cdot; \boldsymbol{\mu})$ with respect to the X-norm, i.e., for all $\boldsymbol{\mu} \in \mathcal{D}$,

$$\alpha_{\mathrm{LB}}(\boldsymbol{\mu}) \le \alpha(\boldsymbol{\mu}) = \inf_{v \in X^{\mathcal{N}}} \frac{a(v, v; \boldsymbol{\mu})}{\|v\|_X^2}. \tag{32}$$

We also define the residual

$$r_N(v; \boldsymbol{\mu}) \equiv f(v; \boldsymbol{\mu}) - a(u_N(\boldsymbol{\mu}), v; \boldsymbol{\mu}) \tag{33}$$

for all $v \in X$. Then, it can be shown that

$$\|u^{\mathcal{N}}(\boldsymbol{\mu}) - u_N(\boldsymbol{\mu})\|_{\boldsymbol{\mu}} \le \frac{\|\hat{e}_N^{\mathcal{N}}(\boldsymbol{\mu})\|_X}{\big(\alpha_{\mathrm{LB}}(\boldsymbol{\mu})\big)^{1/2}} \equiv \Delta_N(\boldsymbol{\mu}), \tag{34}$$

where $\hat{e}_N^{\mathcal{N}}(\boldsymbol{\mu})$ belongs to $X^{\mathcal{N}}$ and satisfies $a(\hat{e}_N^{\mathcal{N}}(\boldsymbol{\mu}), v; \bar{\boldsymbol{\mu}}) = r_N(v; \boldsymbol{\mu})$ for all $v \in X^{\mathcal{N}}$. Thus, $\|\hat{e}_N^{\mathcal{N}}(\boldsymbol{\mu})\|_X = \sup_{v \in X^{\mathcal{N}}} (r_N(v; \boldsymbol{\mu})/\|v\|_X)$ is the dual norm of the residual. Again, due to the affinity assumptions (19), an efficient offline-online computational approach for $\Delta_N(\boldsymbol{\mu})$ can be developed. For a proof of (34) and a detailed derivation of the corresponding computational procedure, we refer to [14].

Now, we let $\tilde{X}^{\mathcal{N}} \supset X^{\mathcal{N}}$ be a discrete FE space identical to $X^{\mathcal{N}}$ except for the restriction on its members vanishing on Γ_{D}^0. Then we let $\psi^{\mathcal{N}}(\boldsymbol{\mu}) \in (V^\star \cap \tilde{X}^{\mathcal{N}})$ be the solution of the problem

$$a(v, \psi^{\mathcal{N}}(\boldsymbol{\mu}); \boldsymbol{\mu}) = 0, \quad \forall v \in X^{\mathcal{N}}. \tag{35}$$

Note that since $\psi^{\mathcal{N}}(\boldsymbol{\mu}) \in (V^\star \cap \tilde{X}^{\mathcal{N}})$, we impose the essential Dirichlet condition $\psi^{\mathcal{N}}|_{\Gamma_{\rm D}^0}(\boldsymbol{\mu}) = 1$.

Next, if we choose any $v^\star \in (V^\star \cap \tilde{X}^{\mathcal{N}})$, our "truth output" – to which the RB output will be compared – is given from (22) as

$$s^{\mathcal{N}}(\boldsymbol{\mu}) = a(u^{\mathcal{N}}(\boldsymbol{\mu}), v^\star; \boldsymbol{\mu}) - f(v^\star; \boldsymbol{\mu}), \tag{36}$$

and we obtain the error estimate

$$\begin{aligned} |s^{\mathcal{N}}(\boldsymbol{\mu}) - s_N(\boldsymbol{\mu}; v^\star)| &= |a(u^{\mathcal{N}}(\boldsymbol{\mu}), v^\star; \boldsymbol{\mu}) - a(u_N(\boldsymbol{\mu}), v^\star; \boldsymbol{\mu})| \\ &= |a(e_N(\boldsymbol{\mu}), v^\star; \boldsymbol{\mu})| \\ &= |a(e_N(\boldsymbol{\mu}), v^\star - \psi^{\mathcal{N}}(\boldsymbol{\mu}); \boldsymbol{\mu})| \\ &\leq \|e_N(\boldsymbol{\mu})\|_{\boldsymbol{\mu}} \|v^\star - \psi^{\mathcal{N}}(\boldsymbol{\mu})\|_{\boldsymbol{\mu}}, \end{aligned} \tag{37}$$

by using the fact that $e_N(\boldsymbol{\mu}) = u^{\mathcal{N}}(\boldsymbol{\mu}) - u_N(\boldsymbol{\mu}) \in X^{\mathcal{N}}$, that $\psi^{\mathcal{N}}(\boldsymbol{\mu})$ and $e_N(\boldsymbol{\mu})$ are orthogonal, and the Cauchy-Schwarz inequality. Thus, $|s^{\mathcal{N}}(\boldsymbol{\mu}) - s_N(\boldsymbol{\mu}; v^\star)| \leq \Delta_N(\boldsymbol{\mu}) \|v^\star - \psi^{\mathcal{N}}(\boldsymbol{\mu})\|_{\boldsymbol{\mu}}$, and a good $v^\star$ is also a good approximation to $\psi^{\mathcal{N}}(\boldsymbol{\mu})$, making the term $\|v^\star - \psi^{\mathcal{N}}(\boldsymbol{\mu})\|_{\boldsymbol{\mu}}$ small.

To bound the term $\|v^\star - \psi^{\mathcal{N}}(\boldsymbol{\mu})\|_{\boldsymbol{\mu}}$, we view $v^\star$ as an approximation to $\psi^{\mathcal{N}}$, and define the residual $r_{v^\star}(\boldsymbol{\mu}) \equiv -a(v^\star, v; \boldsymbol{\mu})$. It can then be shown that

$$\|v^\star - \psi^{\mathcal{N}}(\boldsymbol{\mu})\|_{\boldsymbol{\mu}} \leq \frac{\|\hat{e}_{v^\star}^{\mathcal{N}}(\boldsymbol{\mu})\|_X}{\big(\alpha_{\rm LB}(\boldsymbol{\mu})\big)^{1/2}} \equiv \Delta_{v^\star}(\boldsymbol{\mu}), \tag{38}$$

where $\hat{e}_{v^\star}^{\mathcal{N}}(\boldsymbol{\mu})$ belongs to $X^{\mathcal{N}}$ and solves $a(\hat{e}_{v^\star}^{\mathcal{N}}(\boldsymbol{\mu}), v; \bar{\boldsymbol{\mu}}) = r_{v^\star}(v; \boldsymbol{\mu})$ for all $v \in X^{\mathcal{N}}$ [14]. We thus arrive at

$$|s^{\mathcal{N}}(\boldsymbol{\mu}) - s_N(\boldsymbol{\mu}; v^\star)| \leq \Delta_N(\boldsymbol{\mu}) \Delta_{v^\star}(\boldsymbol{\mu}) \equiv \Delta_{N, v^\star}^{\rm out}(\boldsymbol{\mu}) \tag{39}$$

as an upper bound for our output of interest.

Note that if we write $\psi^{\mathcal{N}}(\boldsymbol{\mu}) = \psi^{\mathcal{N},0}(\boldsymbol{\mu}) + \psi^{\rm D}$, where $\psi^{\rm D} \in (V^\star \cap \tilde{X}^{\mathcal{N}})$ is some chosen Dirichlet lift, we can write (35) as: Given $\boldsymbol{\mu} \in \mathcal{D}$, find $\psi^{\mathcal{N},0}(\boldsymbol{\mu}) \in X^{\mathcal{N}}$ such that

$$a(v, \psi^{\mathcal{N},0}(\boldsymbol{\mu}); \boldsymbol{\mu}) = -a(v, \psi^{\rm D}; \boldsymbol{\mu}), \quad \forall v \in X^{\mathcal{N}}. \tag{40}$$

Thus, if we choose $\psi^{\rm D}$ equal to $v^\star$, (40) is in fact the dual problem corresponding to the *primal* problem (21) with the output functional $l^{\rm out}(\cdot; \boldsymbol{\mu})$ given in (22), since $a(\cdot, v^\star; \boldsymbol{\mu})$ is the linear functional part of $l^{\rm out}(\cdot; \boldsymbol{\mu})$. We elaborate on this in Section 3.5.

3.4 "Good" flux lifting functions

We must keep two things in mind when choosing our flux lifting function $v^\star$. Firstly, it is important that the term $\|v^\star - \psi^{\mathcal{N}}(\boldsymbol{\mu})\|_{\boldsymbol{\mu}}$ in the estimate (37) is

small. Secondly, we must make sure that the computational cost associated with the computation of $v^\star$ is small in the RB online stage.

Note that actually solving (35) for every new $\boldsymbol{\mu}$ and setting $v^\star = \psi^{\mathcal{N}}(\boldsymbol{\mu})$ will result in a zero error in the RB output, but obviously also in an unaffordable "truth FE complexity" online computational cost.

We next consider two alternative choices of "good" $v^\star$'s which both meet the two requirements mentioned above.

3.4.1 Coarse finite element approximation

Our first choice is to construct a coarse finite element approximation to $\psi^{\mathcal{N}}(\boldsymbol{\mu})$. That is to say, we first find $\psi^{\mathcal{M}}(\boldsymbol{\mu}) \in (V^\star \cap \tilde{X}^{\mathcal{M}}) \subset (V^\star \cap \tilde{X}^{\mathcal{N}})$ such that

$$a(v, \psi^{\mathcal{M}}(\boldsymbol{\mu}); \boldsymbol{\mu}) = 0, \quad \forall v \in X^{\mathcal{M}}, \tag{41}$$

where the coarse FE space $\tilde{X}^{\mathcal{M}} \subset \tilde{X}^{\mathcal{N}}$ has $\mathcal{M} \ll \mathcal{N}$ degrees of freedom. We then choose $v^\star = \psi^{\mathcal{M}}(\boldsymbol{\mu})$ as our flux lifting function. In particular, $\mathcal{M}$ should here be chosen small enough that it is affordable to compute $\psi^{\mathcal{M}}(\boldsymbol{\mu})$ in the RB online stage, without compromising the rapid online output evaluation.

Now, to bound the term $\|\psi^{\mathcal{M}}(\boldsymbol{\mu}) - \psi^{\mathcal{N}}(\boldsymbol{\mu})\|_{\boldsymbol{\mu}}$, we use the result (38) to arrive at $\|\psi^{\mathcal{M}}(\boldsymbol{\mu}) - \psi^{\mathcal{N}}(\boldsymbol{\mu})\|_{\boldsymbol{\mu}} \le \Delta_{\mathcal{M}}(\boldsymbol{\mu})$ (we here use $_{\mathcal{M}}$ to indicate that the $v^\star$ in (38) is now a coarse FE approximation to $\psi^{\mathcal{N}}(\boldsymbol{\mu})$). Then, we define $\Delta^{\text{out}}_{N,\mathcal{M}}(\boldsymbol{\mu}) \equiv \Delta_N(\boldsymbol{\mu})\Delta_{\mathcal{M}}(\boldsymbol{\mu})$, and conclude that for all $\boldsymbol{\mu} \in \mathcal{D}$,

$$\left| s^{\mathcal{N}}(\boldsymbol{\mu}) - s_N(\boldsymbol{\mu}; \psi^{\mathcal{M}}(\boldsymbol{\mu})) \right| \le \Delta^{\text{out}}_{N,\mathcal{M}}(\boldsymbol{\mu}). \tag{42}$$

3.4.2 Reference parameter approximation

Alternatively, we may take $v^\star = \psi^{\mathcal{N}}(\bar{\boldsymbol{\mu}})$ as our approximation of $\psi^{\mathcal{N}}(\boldsymbol{\mu})$ for any $\boldsymbol{\mu} \in \mathcal{D}$. Thus, our $v^\star$ is the solution to (35) for the reference parameter, which we precompute in the RB offline stage and reuse every time we evaluate our output of interest, without any additional online cost.

From (38), an upper bound for the term $\|\psi^{\mathcal{N}}(\boldsymbol{\mu}) - \psi^{\mathcal{N}}(\bar{\boldsymbol{\mu}})\|_{\boldsymbol{\mu}}$ is given by $\Delta_{\bar{\boldsymbol{\mu}}}(\boldsymbol{\mu})$ (where we substitute $_{\bar{\boldsymbol{\mu}}}$ for $_{v^\star}$ to remember our particular choice for $v^\star$). We thus get

$$|s^{\mathcal{N}}(\boldsymbol{\mu}) - s_N(\boldsymbol{\mu}; \psi^{\mathcal{N}}(\bar{\boldsymbol{\mu}}))| \le \Delta_N(\boldsymbol{\mu})\Delta_{\bar{\boldsymbol{\mu}}}(\boldsymbol{\mu}) \equiv \Delta^{\text{out}}_{N,\bar{\boldsymbol{\mu}}}(\boldsymbol{\mu}) \tag{43}$$

as an upper bound for the output of interest.

3.5 Primal-dual RB approximation

Evidently, one way to approximate $\psi^{\mathcal{N}}(\boldsymbol{\mu})$ is by way of a reduced basis approximation $\psi_M(\boldsymbol{\mu})$. The RB problem corresponding to (40) (and (35))

reads: Find $\psi_M^0(\boldsymbol{\mu}) \in X_M^{\mathrm{du}}$ such that

$$a(v, \psi_M^0(\boldsymbol{\mu}); \boldsymbol{\mu}) = -a(v, \psi^{\mathrm{D}}; \boldsymbol{\mu}), \quad \forall v \in X_M^{\mathrm{du}}, \tag{44}$$

and set $\psi_M(\boldsymbol{\mu}) = \psi_M^0(\boldsymbol{\mu}) + \psi^{\mathrm{D}}$. Here, X_M^{du} denotes the RB dual approximation space, given by

$$X_M^{\mathrm{du}} = \mathrm{span}\{\psi^{\mathcal{N}}(\boldsymbol{\mu}_m) - \psi^{\mathrm{D}}\}_{m=1}^M, \tag{45}$$

where the $\psi^{\mathcal{N}}(\boldsymbol{\mu}_m)$ are snapshots taken of $\psi^{\mathcal{N}}$ at M different points in parameter space. In fact, the formulation of the two problems (24) and (44), together with the output of interest given in (25), corresponds to a standard RB primal-dual formulation [12, 14], which is the standard way of speeding up the convergence of general non-compliant problems. Let us spend a few lines elaborating on this.

First, we choose a $v^\star \in (V^\star \cap \tilde{X}^{\mathcal{N}})$ and let $\psi^{\mathrm{D}} = v^\star$. The standard "dual-corrected" RB output reads

$$\hat{s}_{M,N}(\boldsymbol{\mu}) \equiv s_N(\boldsymbol{\mu}; \psi^{\mathrm{D}}) - r_N(\psi_M^0(\boldsymbol{\mu}); \boldsymbol{\mu}), \tag{46}$$

where $r_N(v; \boldsymbol{\mu}) = f(v; \boldsymbol{\mu}) - a(u_N(\boldsymbol{\mu}), v; \boldsymbol{\mu})\big)$ is the primal residual and $\psi_M^0(\boldsymbol{\mu})$ is the homogeneous part of the solution to (44). In the below expression, we drop the argument $\boldsymbol{\mu}$ of functions in all intermediate steps for brevity. With $e_N(\boldsymbol{\mu}) = u^{\mathcal{N}}(\boldsymbol{\mu}) - u_N(\boldsymbol{\mu})$, we see that

$$\begin{aligned}
|s^{\mathcal{N}}(\boldsymbol{\mu}) - \hat{s}_{M,N}(\boldsymbol{\mu})| &= |s^{\mathcal{N}}(\boldsymbol{\mu}) - s_N(\boldsymbol{\mu}; \psi^{\mathrm{D}}) + r_N(\psi_M^0; \boldsymbol{\mu})| \\
&= |a(e_N, \psi^{\mathrm{D}}; \boldsymbol{\mu}) + r_N(\psi_M^0; \boldsymbol{\mu})| \\
&= |a(e_N, \psi^{\mathcal{N},0}; \boldsymbol{\mu}) - r_N(\psi_M^0; \boldsymbol{\mu})| \\
&= |a(e_N, \psi^{\mathcal{N},0}; \boldsymbol{\mu}) - a(u_N, \psi_M^0; \boldsymbol{\mu}) + f(\psi_M^0; \boldsymbol{\mu})| \\
&= |a(e_N, \psi^{\mathcal{N},0}; \boldsymbol{\mu}) - a(u_N, \psi_M^0; \boldsymbol{\mu}) + a(u^{\mathcal{N}}, \psi_M^0; \boldsymbol{\mu})| \\
&= |a(e_N, \psi^{\mathcal{N},0} - \psi_M^0; \boldsymbol{\mu})| \\
&\leq \|e_N\|_{\boldsymbol{\mu}}(\boldsymbol{\mu}) \|\psi^{\mathcal{N},0}(\boldsymbol{\mu}) - \psi_M^0(\boldsymbol{\mu})\|_{\boldsymbol{\mu}},
\end{aligned} \tag{47}$$

where we in the first step use the arbitrarity (up to functions in $(V^\star \cap \tilde{X}^{\mathcal{N}})$) of the flux lifting function for the "truth" output, and thus $s^{\mathcal{N}}(\boldsymbol{\mu}) - \hat{s}_{M,N}(\boldsymbol{\mu}; \psi^{\mathrm{D}}) = a(e_N(\boldsymbol{\mu}), \psi^{\mathrm{D}}; \boldsymbol{\mu})$ is precisely the right-hand-side of (40) for $v = -e_N(\boldsymbol{\mu})$. Hence, if we solve the RB primal and dual problems in parallel with $M \approx N$, we get a quadratic effect in the convergence of the output of interest.

Next, it is straightforward to deduce that $\hat{s}_{M,N}(\boldsymbol{\mu}) = s_N(\boldsymbol{\mu}; \psi_M(\boldsymbol{\mu}))$, i.e., that these two output evaluations are equivalent. We start with the expression (46), and then appeal to the (bi)linearity of $a(\cdot, \cdot; \boldsymbol{\mu})$ and $f(\cdot, \boldsymbol{\mu})$.

Again, we drop the $\boldsymbol{\mu}$-dependence of functions for typesetting convenience:

$$\begin{aligned}\hat{s}_{M,N}(\boldsymbol{\mu}) &= s_N(\boldsymbol{\mu};\psi^{\mathrm{D}}) - r_N(\psi_M^0;\boldsymbol{\mu}) \\ &= a(u_N;\psi^{\mathrm{D}};\boldsymbol{\mu}) + a(u_N,\psi_M^0;\boldsymbol{\mu}) - f(\psi^{\mathrm{D}};\boldsymbol{\mu}) - f(\psi_M^0;\boldsymbol{\mu}) \\ &= a(u_N;\psi^{\mathrm{D}}+\psi_M^0) - f(\psi^{\mathrm{D}}+\psi_M^0;\boldsymbol{\mu}) \\ &= s_N(\boldsymbol{\mu};\psi_M). \end{aligned} \tag{48}$$

In other words, the standard dual-corrected output with $v^\star = \psi^{\mathrm{D}}$ produces the same result as the non-corrected output with $v^\star = \psi_M(\boldsymbol{\mu})$. Thus, for flux integral outputs, the standard RB primal-dual approximation framework may be viewed as a technique for improving upon any initial choice made for $v^\star$. Hence, we recognise $v^\star$ as the Dirichlet lifting function for the dual problem.

Up to this point, we have only considered a single output of interest. Surely, it could in a practical application be desirable to evaluate several outputs of interest, all being functionals of the solution of the same underlying PDE. For example, we might want the flux through K distinct parts $\Gamma_{\mathrm{D}}^0, \Gamma_{\mathrm{D}}^1, \ldots, \Gamma_{\mathrm{D}}^{K-1}$ of the boundary, resulting in K different output functionals and thus in turn K different dual problems. Of coarse, in the case of multiple outputs, no more than one can be compliant.

When K is small, solving the primal and dual problems in parallel with (say) $M \approx N$ basis functions may drastically reduce the RB output error(s) and error bound(s). However, for many outputs (large K), online computation of the solution to every corresponding dual problem (when $M \approx N$) may be impracticable – $\mathcal{O}(N^3)$ and $\mathcal{O}(M^3)$ operations are required for direct computation of the solutions to the primal and dual RB problems, respectively – and we are thus forced to trade numerical accuracy for computational speed. In this situation, choosing good flux lifting functions seems important. On the other hand, if we do proceed with RB approximations to the solution(s) to the dual problem(s) as well, making good choices for the dual Dirichlet liftings would surely be of interest (obviously, $\psi^{\mathrm{D}} = \psi^{\mathcal{N}}(\boldsymbol{\mu})$ would be the optimal, though an impractical, choice).

3.6 Computational approach for output evaluation

In the RB online stage, and without regard to our particular choice for $v^\star$, we need to compute

$$s_N(\boldsymbol{\mu}) = l^{\mathrm{out}}(u_N(\boldsymbol{\mu})) = a(u_N(\boldsymbol{\mu}), v^\star;\boldsymbol{\mu}) - f(v^\star;\boldsymbol{\mu}), \tag{49}$$

once the RB solution coefficients are obtained. Note that also when we pursue a primal-dual approximation, we are still left with an evaluation on this form, due to the result (48).

Since, for $\boldsymbol{\mu} \in \mathcal{D}$, $a(\cdot,\cdot;\boldsymbol{\mu})$ and $f(\cdot;\boldsymbol{\mu})$ are linear and, by assumption, affine, $l^{\mathrm{out}}(\cdot;\boldsymbol{\mu})$ will also be linear and affine (i.e., affine in functions of $\boldsymbol{\mu}$).

Hence, we can compute the RB output at an additional computational cost of $\mathcal{O}(N)$ operations. To see this, we write $a(v, w; \boldsymbol{\mu})$ and $f(v; \boldsymbol{\mu})$ in their affine expansions (19) as

$$a(v, w; \boldsymbol{\mu}) = \sum_{q=1}^{Q_a} a^q(v, w)\Theta_a^q(\boldsymbol{\mu}), \qquad f(v; \boldsymbol{\mu}) = \sum_{q=1}^{Q_f} f^q(v)\Theta_f^q(\boldsymbol{\mu}), \tag{50}$$

for any $v, w \in X$. With $u_N(\boldsymbol{\mu}) = \sum_{n=1}^{N} u_{N,n}(\boldsymbol{\mu})\zeta_n$, where the ζ_n are the orthogonalised RB basis functions (in order to get a reduced system of equations that is well conditioned, the basis functions $u^{\mathcal{N}}(\boldsymbol{\mu}_n)$, $1 \le n \le N$, are orthogonalised with respect to the norm $\|\cdot\|_X$, c.f. [14]) and $u_{N,n}(\boldsymbol{\mu})$ are the RB solution coefficients, we get

$$\begin{aligned} l^{\text{out}}(u_N(\boldsymbol{\mu})) &= \sum_{q=1}^{Q_a} a^q(u_N(\boldsymbol{\mu}), v^\star)\Theta_a^q(\boldsymbol{\mu}) - \sum_{q=1}^{Q_f} f^q(v^\star)\Theta_f^q(\boldsymbol{\mu}) \\ &= \sum_{n=1}^{N} u_{N,n}(\boldsymbol{\mu}) \sum_{q=1}^{Q_a} a^q(\zeta_n, v^\star)\Theta_a^q(\boldsymbol{\mu}) - \sum_{q=1}^{Q_f} f^q(v^\star)\Theta_f^q(\boldsymbol{\mu}), \end{aligned} \tag{51}$$

which is a $Q_a N + Q_f$ operations summation, assuming that the values $a^q(\zeta_n, v^\star)$, $1 \le q \le Q_a$, and $f^q(v^\star)$, $1 \le q \le Q_f$ are precomputed in the RB offline stage, and that the function values $\Theta_a^q(\boldsymbol{\mu})$ and $\Theta_f^q(\boldsymbol{\mu})$ are readily computable.

In the more general case of a non-affine problem, we can construct affine expansions that are good approximations of $a(\cdot, \cdot; \boldsymbol{\mu})$ and $f(\cdot; \boldsymbol{\mu})$ for any $\boldsymbol{\mu} \in \mathcal{D}$ by invoking the *empirical interpolation* method [3, 8]. In this case, the computational cost for output evaluation is still only $\mathcal{O}(N)$ in the RB online stage, but for a slightly modified problem.

4 An Illustrative Example

4.1 Problem formulation

We consider the electrostatic potential u inside a square domain Ω which contains an "insulating" anomaly, Ω_{an}, as depicted in Figure 2. Attached to the boundary of Ω, $\partial\Omega$, are four electrodes, which constitute the Dirichlet boundary $\Gamma_{\text{D}} \equiv \Gamma_{\text{south}} \cup \Gamma_{\text{north}} \cup \Gamma_{\text{east}} \cup \Gamma_{\text{west}}$. Here, the electrostatic potential is prescribed as

$$u = \begin{cases} 1, & \text{on } \Gamma_{\text{south}}, \\ 0, & \text{on } \Gamma_{\text{north}} \cup \Gamma_{\text{east}} \cup \Gamma_{\text{west}}. \end{cases} \tag{52}$$

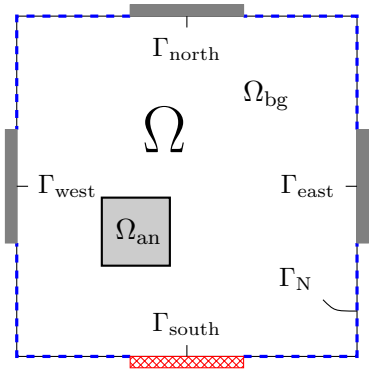

Figure 2: Physical domain Ω with an electrode attached to each edge.

On the Neumann boundary, $\Gamma_{\text{N}} \equiv \partial\Omega \setminus \Gamma_{\text{D}}$, we assume electrostatic insulation, i.e.

$$\frac{\partial u}{\partial n} = 0, \quad \text{on } \Gamma_{\text{N}}. \tag{53}$$

We define the "background material" as $\Omega_{\text{bg}} \equiv \Omega \setminus \overline{\Omega}_{\text{an}}$. The electric permittivity, ϵ, inside Ω is given as

$$\epsilon \equiv \begin{cases} \epsilon_{\text{bg}} \equiv 1, & \text{in } \Omega_{\text{bg}}, \\ \epsilon_{\text{an}} \equiv 0.1, & \text{in } \Omega_{\text{an}}. \end{cases} \tag{54}$$

Finally, in $\Omega_{\text{bg}} \cup \Omega_{\text{an}}$, the electrostatic potential is governed by the Laplace equation,

$$-\Delta u = 0. \tag{55}$$

Our problem is parameterised by the parameter vector $\boldsymbol{\mu} \equiv (\mu_1, \mu_2) \in \mathcal{D} \subset \Omega$, which determines the centre of Ω_{an}. Hence, our domains are parameter-dependent. For typesetting convenience however, we do not explicitly denote this dependence in formulas. Now, with the boundary conditions (52) and (53), together with the assumption of flux continuity on the interior boundary and global continuity of the solution, the parametric weak form of our problem reads: Given $\boldsymbol{\mu} \in \mathcal{D}$ and a lifting u^{D} of the Dirichlet data (52), find $u^0(\boldsymbol{\mu}) \in X$ such that

$$a(u(\boldsymbol{\mu}), v; \boldsymbol{\mu}) = 0, \quad \forall v \in X, \tag{56}$$

where $u(\boldsymbol{\mu}) = u^0(\boldsymbol{\mu}) + u^{\text{D}}$,

$$a(u, v; \boldsymbol{\mu}) = \epsilon_{\text{bg}} \int_{\Omega_{\text{bg}}} \nabla u \cdot \nabla v \, \mathrm{d}\Omega + \epsilon_{\text{an}} \int_{\Omega_{\text{an}}} \nabla u \cdot \nabla v \, \mathrm{d}\Omega \tag{57}$$

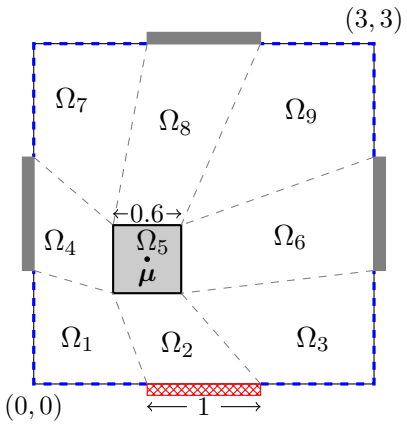

Figure 3: Decomposition of the physical domain into nine (deformed square) spectral elements.

and $X = \{v \in H^1 : v|_{\Gamma_\mathrm{D}} = 0\}$.

Finally, we are interested in evaluating the accumulated charge (capacitance) on the eastern electrode, given by the flux integral

$$\tilde{s}(\boldsymbol{\mu}) \equiv -\epsilon_\mathrm{bg} \int_{\Gamma_\mathrm{east}} \frac{\partial u(\boldsymbol{\mu})}{\partial n} \, \mathrm{d}s. \tag{58}$$

4.2 RB treatment

In order to compute a good set of "truth" snapshots upon which to build our RB approximations, we start our RB treatment by a standard discretisation of (56). To this end, we use a spectral element method based on high order polynomials [10]. Our domain is decomposed into nine spectral elements, as depicted in Figure 3, and we rewrite our problem in terms of the reference variables (ξ, η) on the reference domain $\hat{\Omega} \equiv (-1, 1)^2$ via standard transfinite mappings $\mathcal{F}_i : \Omega_i \rightarrow \hat{\Omega}$ [7]. We may thus write

$$a(u, v; \boldsymbol{\mu}) = \sum_{i=1}^{9} \epsilon_i \int_{\hat{\Omega}} (\hat{\nabla}\hat{u})^\mathrm{T} G_i(\boldsymbol{\mu}) \hat{\nabla}\hat{v} \, \mathrm{d}\hat{\Omega}, \tag{59}$$

where $\hat{v}_i(\xi, \eta) \equiv v(x, y)|_{\Omega_i} \circ \mathcal{F}_i$, and the G_i are parametric and spatial dependent 2×2 matrices comprising geometrical factors.

As our discrete "truth" spaces, we define

$$X^\mathcal{N} \equiv \{v \in H^1(\Omega) : v|_{\Gamma_\mathrm{D}} = 0, \hat{v}_i \in \mathbb{P}_P(\hat{\Omega}), 1 \leq i \leq 9\}, \tag{60}$$

$$\tilde{X}^\mathcal{N} \equiv \{v \in H^1(\Omega) : v|_{\Gamma_\mathrm{D} \setminus \Gamma_\mathrm{east}} = 0, \hat{v}_i \in \mathbb{P}_P(\hat{\Omega}), 1 \leq i \leq 9\}, \tag{61}$$

where $\mathbb{P}_P(\hat{\Omega})$ denotes the space of polynomials of degree P in each direction over $\hat{\Omega}$. As basis functions for $X^\mathcal{N}$, we use the Lagrange polynomials over

the $(P+1)^2$ tensorised GLL nodes [4]. As $\mathcal{N} = \dim(X^{\mathcal{N}})$, we note that $\mathcal{N} \sim P^2$.

Our "truth" problem is thus: Given $\boldsymbol{\mu} \in \mathcal{D}$, find $u^{\mathcal{N},0}(\boldsymbol{\mu}) \in X^{\mathcal{N}}$ such that

$$a(u^{\mathcal{N}}(\boldsymbol{\mu}), v; \boldsymbol{\mu}) = 0, \quad \forall v \in X^{\mathcal{N}}, \tag{62}$$

where $u^{\mathcal{N}}(\boldsymbol{\mu}) = u^{\mathcal{N},0}(\boldsymbol{\mu}) + u^{\mathrm{D}}$ and u^{D} is some chosen lifting of the Dirichlet data (52). As our "truth" output of interest, we take

$$s^{\mathcal{N}}(\boldsymbol{\mu}) = l^{\mathrm{out}}(u^{\mathcal{N}}(\boldsymbol{\mu})) = a(u^{\mathcal{N}}(\boldsymbol{\mu}), v^\star; \boldsymbol{\mu}), \tag{63}$$

for any $v^\star \in (V^\star \cap \tilde{X}^{\mathcal{N}})$, where now

$$V^\star \equiv \{v \in H^1 : v|_{\Gamma_{\mathrm{D}} \setminus \Gamma_{\mathrm{east}}} = 0, v|_{\Gamma_{\mathrm{east}}} = 1\}. \tag{64}$$

In (63), we have omitted the minus sign (that appeared in (58) since the capacitance is positive by definition). Also note that for the "truth" problem, any two $v^\star \in (V^\star \cap \tilde{X}^{\mathcal{N}})$ will produce the same numerical output, as we saw in Section 2.

Our RB problem reads, with the Dirichlet lifting term moved to the right-hand-side, as follows: Given $\boldsymbol{\mu} \in \mathcal{D}$, find $u_N^0(\boldsymbol{\mu}) \in X_N$ such that

$$a(u_N^0(\boldsymbol{\mu}), v; \boldsymbol{\mu}) = -a(u^{\mathrm{D}}, v; \boldsymbol{\mu}), \quad \forall v \in X_N, \tag{65}$$

and set $u_N(\boldsymbol{\mu}) = u_N^0(\boldsymbol{\mu}) + u^{\mathrm{D}}$. We then evaluate our output of interest as

$$s_N(\boldsymbol{\mu}; v^\star) \equiv a(u_N(\boldsymbol{\mu}), v^\star; \boldsymbol{\mu}), \tag{66}$$

where we choose $v^\star \in (V^\star \cap \tilde{X}^{\mathcal{N}})$. For $1 \le N \le N_{\max}$, our RB spaces are defined as

$$X_N \equiv \mathrm{span}\{u_0^{\mathcal{N}}(\boldsymbol{\mu}_n)\}_{n=1}^N, \tag{67}$$

where the $\boldsymbol{\mu}_n$ are chosen greedily based on *a posteriori* upper bounds $\Delta_N(\boldsymbol{\mu})$ for the energy errors $\|u^{\mathcal{N},0}(\boldsymbol{\mu}) - u_N^0(\boldsymbol{\mu})\|_{\boldsymbol{\mu}}$, $1 \le N \le N_{\max}$ [14].

Once a coercivity lower bound $\alpha_{\mathrm{LB}}(\boldsymbol{\mu})$ is established, we can compute an energy-norm error bound $\Delta_N(\boldsymbol{\mu})$ and output error bounds $\Delta_{N,\mathcal{M}}^{\mathrm{out}}(\boldsymbol{\mu})$ and $\Delta_{N,\bar{\boldsymbol{\mu}}}^{\mathrm{out}}(\boldsymbol{\mu})$ as described above (c.f. Sections 3.3, 3.4.1 and 3.4.2). In fact, if we let $\sigma_k(\boldsymbol{\mu})$ denote the set of eigenvalues of the matrix $G_k(\boldsymbol{\mu})$ of geometrical factors, $1 \le k \le 9$, and define

$$\lambda^-(\boldsymbol{\mu}) \equiv \min_{\substack{(\xi,\eta)\in\hat{\Omega} \\ 1\le k\le 9}} \sigma_k(\xi, \eta; \boldsymbol{\mu}), \quad \lambda^+(\boldsymbol{\mu}) \equiv \max_{\substack{(\xi,\eta)\in\hat{\Omega} \\ 1\le k\le 9}} \sigma_k(\xi, \eta; \boldsymbol{\mu}), \tag{68}$$

it can be shown [6] that a coercivity lower bound for our particular problem is given by

$$\alpha_{\mathrm{LB}}(\boldsymbol{\mu}) = \frac{\lambda^-(\boldsymbol{\mu})}{\lambda^+(\bar{\boldsymbol{\mu}})}. \tag{69}$$

We make a remark here that the maximum and minimum of the $\sigma_k(\cdot,\cdot;\boldsymbol{\mu})$ are in practice realised over the tensorised GLL nodes.

Unfortunately, the elements of the matrices G_k will be such that a does not admit an affine expansion as in (19). For this reason the computations do not immediately decouple to offline and online stages. However, as commented in the previous section, the empirical interpolation method provides means to this end [3, 8]. In fact, we can make the empirical interpolation error negligible if we make sure to include enough terms in the approximate affine expansion of a. Moreover, the additional term in the *a posteriori* error estimators that accounts for the empirical interpolation error (see [3, 11]) will vanish as the interpolation error goes to zero. Hence, under the assumption of a negligible interpolation error, the estimators above are still valid. However, in the numerical tests that follow, we have chosen to not use an offline-online decoupling approach, since this is not critical for our conclusions.

4.3 Numerical results

Define the RB output error

$$e_N^{\text{out}}(\boldsymbol{\mu}; v^\star) \equiv |s_N(\boldsymbol{\mu}; v^\star) - s^{\mathcal{N}}(\boldsymbol{\mu})|. \tag{70}$$

For $v^\star \in (V^\star \cap \tilde{X}^{\mathcal{N}})$, we shall make use of three different functions: The reference parameter approximation $\psi^{\mathcal{N}}(\bar{\boldsymbol{\mu}})$ discussed in 3.4.2, the coarse finite element approximation $\psi^{\mathcal{M}_2}(\boldsymbol{\mu})$ discussed in 3.4.1, which corresponds to the solution of (41) using polynomials of second degree as basis functions, and a "naive" choice, $v^\star_{\text{naive}}$, given as

$$v^\star_{\text{naive}} \equiv \begin{cases} 1, & \text{on } \Gamma_{\text{east}}, \\ 0, & \text{at every other GLL node.} \end{cases} \tag{71}$$

Note that in a spectral element context, the naive choice would be the natural and computationally convenient choice to make for $v^\star$.

We also introduce a test sample $\Xi_{\text{test}} \subset \mathcal{D}$ consisting of 200 randomly distributed points.

In Figure 4, we plot the maximum (to the left) and mean (to the right) of the output errors $e_N^{\text{out}}(\boldsymbol{\mu}; \psi^{\mathcal{N}}(\bar{\boldsymbol{\mu}}))$, $e_N^{\text{out}}(\boldsymbol{\mu}; \psi^{\mathcal{M}_2}(\boldsymbol{\mu}))$ and $e_N^{\text{out}}(\boldsymbol{\mu}; v^\star_{\text{naive}})$ over all $\boldsymbol{\mu} \in \Xi_{\text{test}}$ as a function of the number reduced basis functions, N. We conclude that the two "good" choices for $v^\star$ in general perform about an order of magnitude better than the naive choice.

Next, for all $\boldsymbol{\mu} \in \Xi_{\text{test}}$, and for the particular case of $N = 25$, we compute the *effectivity* associated with our output error estimator $\Delta^{\text{out}}_{N,\bar{\boldsymbol{\mu}}}$, defined as

$$\nu^{\text{out}}_{N,\bar{\boldsymbol{\mu}}}(\boldsymbol{\mu}) \equiv \frac{\Delta^{\text{out}}_{N,\bar{\boldsymbol{\mu}}}(\boldsymbol{\mu})}{e_N^{\text{out}}(\boldsymbol{\mu}; \psi^{\mathcal{N}}(\bar{\boldsymbol{\mu}}))}. \tag{72}$$

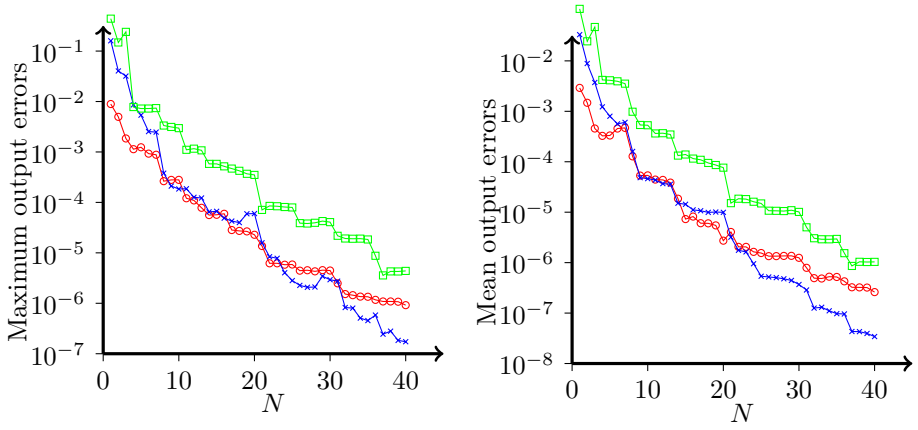

Figure 4: Maximum (left) and mean (right) of the output errors $e_N^{\mathrm{out}}(\boldsymbol{\mu}; v^\star)$ over Ξ_{test} for the three choices $\psi^{\mathcal{N}}(\bar{\boldsymbol{\mu}})$ ($\times$), $\psi^{\mathcal{M}_2}(\boldsymbol{\mu})$ ($\circ$) and $v^\star_{\mathrm{naive}}$ ($\square$) for $v^\star$, as functions of the number of reduced basis functions, N.

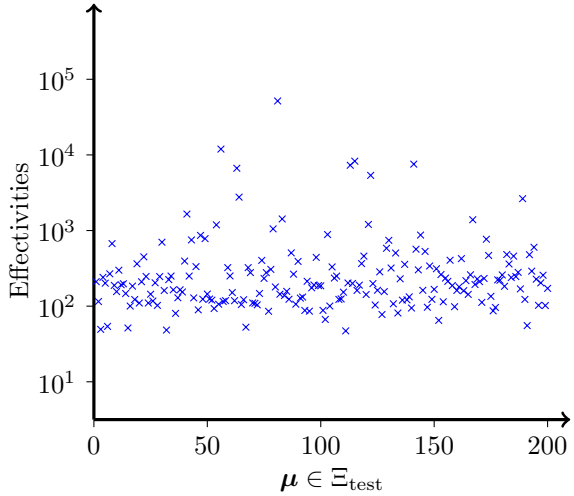

Figure 5: Output error bound effectivity $\nu^{\mathrm{out}}_{N,\bar{\boldsymbol{\mu}}}(\boldsymbol{\mu})$ for all $\boldsymbol{\mu} \in \Xi_{\mathrm{test}}$ for $N = 25$ (in no particular order).

Associated with the other two choices for $v^\star$, we define the effectivities $\nu^{\text{out}}_{N,\mathcal{M}_2}(\boldsymbol{\mu})$ and $\nu^{\text{out}}_{N,v^\star_{\text{naive}}}(\boldsymbol{\mu})$ in a similar way. For most $\boldsymbol{\mu} \in \Xi_{\text{test}}$, the effectivity $\nu^{\text{out}}_{N,\bar{\boldsymbol{\mu}}}(\boldsymbol{\mu})$ is in the range $\mathcal{O}(100) < \nu^{\text{out}}_{N,\bar{\boldsymbol{\mu}}}(\boldsymbol{\mu}) < \mathcal{O}(1000)$, as shown in Figure 5. For the other two effectivities, $\nu^{\text{out}}_{N,\mathcal{M}_2}(\boldsymbol{\mu})$ and $\nu^{\text{out}}_{N,v^\star_{\text{naive}}}(\boldsymbol{\mu})$, the results are similar (not shown). We also find that, for most $\boldsymbol{\mu} \in \Xi_{\text{test}}$, $\nu^{\text{out}}_{N,\mathcal{M}_2}(\boldsymbol{\mu}) < \nu^{\text{out}}_{N,\bar{\boldsymbol{\mu}}}(\boldsymbol{\mu}) < \nu^{\text{out}}_{N,v^\star_{\text{naive}}}(\boldsymbol{\mu})$. This is, however, not generally true for other choices of N.

The reason for the output error estimators being rather conservative is the large "angle" between the error of the primal problem, $u_N(\boldsymbol{\mu}) - u^{\mathcal{N}}(\boldsymbol{\mu})$, and the error of the dual problem, $\psi^{\mathcal{N}}(\bar{\boldsymbol{\mu}}) - \psi^{\mathcal{N}}(\boldsymbol{\mu})$. Thus, the Cauchy-Schwarz inequality, used in (37), becomes unsharp. This point is readily verified for the estimator $\Delta^{\text{out}}_{N,\bar{\boldsymbol{\mu}}}$ by separate computation of the effectivities associated with the estimators $\Delta_N(\boldsymbol{\mu})$ and $\Delta_{\bar{\boldsymbol{\mu}}}(\boldsymbol{\mu})$ for the primal and dual problems, respectively, which are indeed close to unity (of course, the same argument works for the other estimators as well). For $N = 25$, we find

$$\max_{\boldsymbol{\mu}\in\Xi_{\text{test}}} \frac{\Delta_N(\boldsymbol{\mu})}{\|u_N(\boldsymbol{\mu}) - u^{\mathcal{N}}(\boldsymbol{\mu})\|_{\boldsymbol{\mu}}} \approx 2.68 \tag{73}$$

and (irrespective of N)

$$\max_{\boldsymbol{\mu}\in\Xi_{\text{test}}} \frac{\Delta_{\bar{\boldsymbol{\mu}}}(\boldsymbol{\mu})}{\|\psi^{\mathcal{N}}(\bar{\boldsymbol{\mu}}) - \psi^{\mathcal{N}}(\boldsymbol{\mu})\|_{\boldsymbol{\mu}}} \approx 2.94. \tag{74}$$

Hence, we do have a quite sharp bound for the right hand side of (37) for all $\boldsymbol{\mu} \in \Xi_{\text{test}}$, and the unsharpness of the RB output error bound must be ascribed to the Cauchy-Schwarz inequality. Another implication of the sharpness of the individual error bounds is that our coercivity lower bound, $\alpha_{\text{LB}}(\boldsymbol{\mu})$, must be very sharp for all $\boldsymbol{\mu} \in \Xi_{\text{test}}$.

4.4 A note on a special compliant problem

For the Laplace equation (55), the corresponding bilinear form $a(\cdot,\cdot;\boldsymbol{\mu})$ is symmetric, and the only term that enters on the right-hand-side in the weak formulation, e.g. (65), is the Dirichlet lifting term $-a(u^{\text{D}}, v; \boldsymbol{\mu})$. Now, in the very special case that we would like to evaluate the flux integral output over the same electrode on which a unity potential was imposed, we may choose $v^\star = u^D$ as the flux lifting function. In this case, our RB output of interest is $s_N(\boldsymbol{\mu}; u^{\text{D}}) = a(u_N(\boldsymbol{\mu}), u^{\text{D}}; \boldsymbol{\mu})$. With $e_N(\boldsymbol{\mu}) = u^{\mathcal{N}}(\boldsymbol{\mu}) - u_N(\boldsymbol{\mu})$, we get

$$\begin{aligned} |s^{\mathcal{N}}(\boldsymbol{\mu}) - s_N(\boldsymbol{\mu}; u^{\text{D}})| &= |a(e_N(\boldsymbol{\mu}), u^{\text{D}}; \boldsymbol{\mu})| \\ &= |a(u^{\text{D}}, e_N(\boldsymbol{\mu}); \boldsymbol{\mu})| \\ &= |a(u^{\mathcal{N}}(\boldsymbol{\mu}), e_N(\boldsymbol{\mu}); \boldsymbol{\mu})| \\ &= |a(e_N(\boldsymbol{\mu}), e_N(\boldsymbol{\mu}); \boldsymbol{\mu})| = \|e_N(\boldsymbol{\mu})\|^2_{\boldsymbol{\mu}}, \end{aligned} \tag{75}$$

where we use the symmetry of $a(\cdot,\cdot;\boldsymbol{\mu})$, then (56) and the fact that $e_N(\boldsymbol{\mu}) \in X^{\mathcal{N}}$, and finally again symmetry of $a(\cdot,\cdot;\boldsymbol{\mu})$ and Galerkin orthogonality. Hence, the RB output error converges quadratically with the energy-norm error without any simultaneous primal-dual treatment.

In the multi-electrode case, it is of little practical interest to evaluate the capacitance over the electrode with unity Dirichlet data, since this evaluation would only yield the *total* capacitance, as if we were to sum up the capacitances between the selected electrode and each of the other electrodes. However, for the sake of argument, suppose our system consists of only two electrodes. Then the exact output over one of the electrodes is equal to the exact output over the other, with a minus sign. We can thus choose to evaluate the output over the electrode with unity Dirichlet data (and multiply by (-1)).

We emphasise again that this compliant effect is restricted to the special case in which $f = 0$, the unity Dirichlet input electrode coincides with the output electrode and $a(\cdot,\cdot;\boldsymbol{\mu})$ is symmetric.

We end this section referring to [6], where the numerical example discussed in this section is extended to incorporate three outputs (specifically, the capacitances between the south electrode, Γ_{south}, and each of the other electrodes, Γ_{east}, Γ_{north} and Γ_{west}). Also, several symmetries of the problem are exploited, which we have not done in this paper for the sake of simplicity of exposition.

5 Concluding Remarks

We have shown that the flux lifting function $v^\star$ should be chosen with care when evaluating flux integral outputs from reduced basis approximations. Our two different proposals for a "good" $v^\star$ have been seen to give better results (a smaller output error) than a naive $v^\star$ in a simple (Laplace equation) numerical example. We note that the naive $v^\star$ would have performed equally well as the "good" ones within a standard finite element context, due to the richness of the FE approximation space (in fact, the naive choice is convenient in terms of implementation, and is thus often used in practice for the FE method).

In the case of many (flux integral) outputs of interest that are all functionals of the same RB solution, a standard primal-dual error reduction technique may become too expensive. In this case, choosing a good $v^\star$ is important to make sure that the RB (primal only) output error is not unnecessarily large.

Acknowledgements

We would like to thank Professor Anthony T. Patera of M.I.T., and Dr D.B.P. Huynh for the many helpful comments and suggestions recieved throughout

the work on this paper.

References

[1] I. Babuška and A. Miller. The post-processing approach in the finite element method – Part 1: Calculation of displacements, stresses and other higher derivatives of the displacements. *Internat. J. Numer. Methods Engrg.*, 20:1085–1104, 1984.

[2] I. Babuška and M. Suri. The p and h-p versions of the finite element method, basic principles and properties. *SIAM Rev.*, 36(4):578–632, 1994.

[3] M. Barrault, Y. Maday, N. C. Nguyen, and A. T. Patera. An 'empirical interpolation' method: application to efficient reduced-basis discretization of partial differential equations. *C. R. Math. Acad. Sci. Paris*, 339(9):667–672, 2004.

[4] C. Bernardi and Y. Maday. Spectral methods. In *Handbook of numerical analysis, Vol. V*, Handb. Numer. Anal., V, pages 209–485. North-Holland, Amsterdam, 1997.

[5] G. F. Carey. Derivative calculation from finite element solutions. *Comput. Methods Appl. Mech. Engrg.*, 35(1):1–14, 1982.

[6] J. L. Eftang. Reduced basis methods for partial differential equations. Master's thesis, Norwegian University of Science and Technology, 2008.

[7] W. J. Gordon and C. A. Hall. Construction of curvilinear co-ordinate systems and applications to mesh generation. *Internat. J. Numer. Methods Engrg.*, 7:461–477, 1973.

[8] M. A. Grepl, Y. Maday, N. C. Nguyen, and A. T. Patera. Efficient reduced-basis treatment of nonaffine and nonlinear partial differential equations. *M2AN Math. Model. Numer. Anal.*, 41(3):575–605, 2007.

[9] P. M. Gresho, R. L. Lee, R. L. Sani, M. K. Maslanik, and B. E. Eaton. The consistent galerkin FEM for computing derived boundary quantities in thermal and/or fluids problems. *International journal for numerical mehods in fluids*, 7:371–394, 1987.

[10] Y. Maday and A. T. Patera. Spectral element methods for the Navier-Stokes equations. In A.K. Noor and J.T. Oden, editors, *State of the art surveys in Computational Mechanics*, pages 71–143. ASME, 1989.

[11] N. C. Nguyen. *Reduced-Basis Approximations and* A Posteriori *Error Bounds for Nonaffine and Nonlinear Partial Differential Equations:*

Application to Inverse Analysis. PhD thesis, Singapore-MIT Alliance, National University of Singapore, 2005.

[12] C. Prud'homme, D. V. Rovas, K. Veroy, L. Machiels, Y. Maday, A. T. Patera, and G. Turinici. Reliable real-time solution of parametrized partial differential equations: Reduced-basis output bound methods. *Journal of Fluids Engineering*, 124(1):70–80, 2002.

[13] A. Quarteroni and A. Valli. *Numerical approximation of partial differential equations*, volume 23 of *Springer Series in Computational Mathematics*. Springer-Verlag, Berlin, 1994.

[14] G. Rozza, D. B. P. Huynh, and A. T. Patera. Reduced basis approximation and *a Posteriori* error estimation for affinely parametrized elliptic coercive partial differential equations. *Archives of Computational Methods in Engineering*, 15(3):229–275, 2008.